

# Are the halo occupation predictions consistent with large scale clustering in galaxy simulations?

Arnaud Pujol\*, Enrique Gaztañaga

*Institut de Ciències de l'Espai (ICE, IEEC/CSIC), E-08193 Bellaterra (Barcelona), Spain*

Accepted xxxx. Received xxx

## ABSTRACT

We study how well we can reconstruct the 2-point clustering of galaxies on linear scales, as a function of mass and luminosity, using the halo (and subhalo) occupation distribution (HOD) in several semi-analytical models of galaxy formation from the Millennium Simulation. In general we find that the reconstruction works at best to  $\simeq 5\%$  accuracy: it underestimates (overestimates) the bias for bright (faint) galaxies. We find that HOD with Friends of Friends groups can reproduce galaxy clustering better than gravitationally bound haloes (main haloes). This indicates that Friends of Friends groups are more directly related to the clustering of these regions than the bound particles in spherical overdensities. However, the reconstruction does not work using subhaloes. This effect is due to the strong environmental dependence on the host halo substructure that distorts the mass dependence of subhalo clustering. We have also found that the reconstructions of galaxy bias from the HOD model fails for low mass haloes with  $M \lesssim 10^{11} h^{-1} M_{\odot}$ . We find that this is because galaxy clustering in these simulations does not seem to depend strongly on halo mass for these low masses.

**Key words:** galaxy clustering; large-scale structure of the Universe.

## 1 INTRODUCTION

Understanding the link between galaxies and dark matter is one of the fundamental problems that makes precision cosmology difficult to reach. Nowadays cosmological simulations provide accurate measurements of the dark matter distribution of the Universe, but we need to relate the dark matter to galaxy distributions in order to compare to observations.

There are several empirical models of galaxy formation that allow us to populate dark matter simulations with galaxies. On one side, the Halo Occupation Distribution (HOD) (e.g. Berlind & Weinberg 2002) formalism uses the Halo Model (e.g. Cooray & Sheth 2002) to describe the population of galaxies according to the probability  $P(N|M)$  that a halo of virial mass  $M$  contains  $N$  galaxies of a given type. This model assumes that the properties of galaxies only depend on the mass of the host halo, and one can then calculate galaxy clustering from the combination of HOD with the clustering of halos. Sheth et al. (2001) used the GIF simulations (Kauffmann et al. 1999) to model the 2-point

clustering of galaxies from the clustering of haloes and the HOD. They found a good agreement with semi-analytical models.

If the HOD assumptions are correct we can use galaxy surveys to obtain the relations between properties of galaxies and halo mass, to measure the clustering of dark matter haloes, as well as halo masses (Zehavi et al. 2005, Zheng, Coil and Zehavi 2007, Zehavi et al. 2011, Coupon et al. 2012, Geach et al. 2012). Skibba et al. (2006) used the halo model assumptions from Zehavi et al. (2005) to study the relation between halo mass and satellite and central luminosities, finding a strong relation between central galaxy luminosities and halo mass, and weak dependence for the satellite galaxies. Moster et al. (2010) assumed the HOD to study the relation between the stellar mass of galaxies and halo mass, finding agreement with galaxy clustering in the SDSS. Kravtsov et al. (2004) found a relation between the halo mass dependence of populations of subhaloes and the HOD of baryonic simulations and semi-analytical models of galaxies, an indication that the distribution of galaxies can be closely related to the distribution of subhaloes.

However, some studies indicate that several properties of galaxy and halo clustering depend on properties of dark

\* E-mail: pujol@ice.cat

matter haloes other than mass, such as halo formation time, density concentration or subhalo occupation number (Gao et al. 2005, Wechsler et al. 2006, Croft et al. 2012). Wechsler et al. (2006) also saw that the dependence of halo clustering on halo formation time changes with mass. Croft et al. (2012) studied the clustering dependence of haloes on the occupation number of subhaloes, and found that for fixed masses, the halo bias depends strongly on the number of subhaloes per halo. They found that, for fixed occupation number of subhaloes, the halo bias depends on mass. They also found a strong anticorrelation between clustering and mass for highly occupied haloes. As galaxies possibly follow subhalo gravitational potentials, this dependence can also be found for galaxies, as we show in §4.1.

Another common technique is the Subhalo Abundance Matching (SHAM), which relates monotonically one property of galaxies to another property of subhaloes, populating each subhalo with at most one galaxy. Reddick et al. (2012) used the Bolshoi simulation to study different methods of SHAM comparing them to SDSS through galaxy clustering, finding  $v_{max,peak}$  of subhaloes to be the best indicator for galaxy clustering. On the other hand, Hearin et al. (2012) found inconsistencies for SHAM when trying to reproduce galaxy clustering and group multiplicity function at the same time.

Finally, semi-analytical models (SAM) populate galaxies in the dark matter haloes by modelling baryonic processes such as gas cooling, disk formation, star formation, supernova feedback, reionization, ram pressure or dust extinction (Cole et al. 2000, Baugh 2006, Baugh 2013) according to the potentials of dark matter. These processes contain free parameters that can be constrained by observations. Because of these processes, semi-analytical models of galaxy formation follow the evolution of the dark matter haloes, mergers, and they are more physical than HOD or SHAM models in terms of environmental dependences and evolution.

In this paper we want to study the consistency of the HOD model in SAMs by focusing on the luminosity dependence of galaxy clustering at large scales. We use the Millennium Simulation (Springel et al. 2005) to measure the halo and subhalo bias. We also compare different definitions of halo. We study the public SAMs of galaxies of the Millennium Simulation to see if we can reproduce the galaxy bias from the HOD model, thereby assuming that the clustering of galaxies only depends on the mass of the host halo. We do this by measuring both the halo bias and the HOD in the same simulation and for the same galaxies that we want to reproduce the bias. This analysis is similar to that of Sheth et al. (2001) but with some important differences. First of all, Sheth et al. (2001) model the halo bias, while we use the measurement in the simulation, and we also compare it to modelling the bias. Moreover, we include the errors of the reconstructions of galaxy clustering in order to see numerically their success. Another difference with the study of Sheth et al. (2001) is that we study several and newer SAMs in order to compare the results between them. Finally, the Millennium Simulation presents a better resolution than GIF simulations and therefore we can study smaller masses,

and larger volume so we can study the 2-halo term properly. We also focus on large scales, where no assumptions are needed for the distribution of galaxies inside the haloes. Sheth et al. (2001) assumed the galaxies to be tracers of dark matter particles of the haloes, an assumption which has an impact on the 1-halo term of the 2-point clustering. Here we only look at the 2-halo term. We also analyse the clustering dependence of the halo occupation of subhaloes, and its dependence on halo mass.

The paper is organized as follows. In §2 we introduce the Millennium Simulation as well as the semi-analytical models of galaxy formation. In §3 we present the measurements of galaxy and halo bias and the HODs that we use to reconstruct the galaxy bias and compare it to the measurements in the simulation, which is developed in §4. We finish with a summary and discussion in §5.

## 2 SIMULATION DATA

For our study we use the Millennium Simulation (Springel et al. 2005), carried out by the Virgo Consortium using the GADGET2 (Springel et al. 2001) code with the TREE-PM (Xu 1995) algorithm to compute the gravitational interaction. The simulation corresponds to a  $\Lambda$ CDM cosmology with the parameters:  $\Omega_m = \Omega_{dm} + \Omega_b = 0.25$ ,  $\Omega_b = 0.045$ ,  $h = 0.73$ ,  $\Omega_\Lambda = 0.75$ ,  $n = 1$  and  $\sigma_8 = 0.9$ . It contains  $2160^3 = 10,077,696,000$  particles of mass  $8.6 \times 10^8 h^{-1} M_\odot$  in a comoving box of size  $500 h^{-1}$  Mpc, with a spatial resolution of  $5 h^{-1}$  Kpc. The Boltzmann code CMBFAST (Seljak & Zaldarriaga 1996) has been used to compute the initial conditions based on WMAP (Spergel et al. 2003) and 2 degree Field Galaxy Redshift Survey (2dFGRS) data (Cole et al. 2005). The simulation output starts at  $z = 127$  and it has 64 snapshots from this time to  $z = 0$ .

### 2.1 Haloes

In each snapshot, the haloes are identified as Friends-of-Friends (FOF) groups with a linking length of 0.2 times the mean particle separation. All the FOF with fewer than 20 particles are discarded. Finally, subhaloes are identified in the FOF groups using the SUBFIND (Springel et al. 2001) algorithm, discarding all the subhaloes with fewer than 20 particles. The main subhalo found in the FOF is located in its centre, and usually has approximately the 90% of the FOF mass. For this reason, it is sometimes called the *main halo*. Throughout this paper, we refer to the FOF groups as the *haloes*, the main SUBFIND object of each FOF is called the *main halo*, and the *subhaloes* refer to all the SUBFIND objects found (including the main haloes). We must notice that these halo and subhalo catalogues are independent of the galaxy catalogues of the simulation. In Fig. 1 we show the mass function of haloes, main haloes and subhaloes, in purple, cyan and red lines respectively, compared to the theoretical models of Tinker et al. (2008) and Sheth, Mo & Tormen (2001) (hereafter SMT 2001). The mass function has been multiplied by  $M^2/\bar{\rho}$  for clarity. We define the masses as the total number of particles belonging to the FOF for

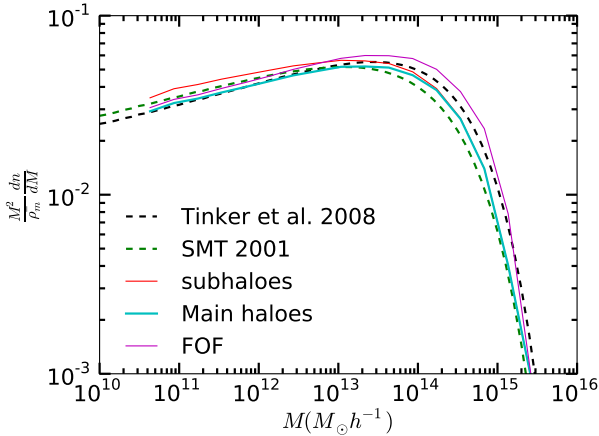


**Figure 1.** Normalized Mass Function of haloes (purple), main haloes (cyan) and subhaloes (red) compared to theoretical models. Black dashed line represent the theoretical mass function from Tinker et al. 2008. Green dashed line shows the model from Sheth, Mo & Tormen 2001.

the haloes, and the total number of particles belonging to each SUBFIND object in the case of the main haloes and subhaloes. We can see that the main haloes have a mass function close to the model of SMT 2001, where the ellipsoidal collapse model has been used. On the other hand, the mass function of haloes is closer to the model of Tinker et al. (2008). We can also see that the mass function of main haloes is very close to the one of haloes at low masses, meaning that most of the small main haloes are contained in small FOFs, while at large masses the mass function of main haloes tends to those of subhaloes, meaning that most of the large subhaloes are main haloes. As a final observation, there are more small subhaloes than haloes and more large haloes than subhaloes, as expected. This is important to understand the relation between the reconstructions of galaxy bias (Figs. 8, 9 and 10) and Figures 14 and 16.

## 2.2 Galaxies

Galaxy catalogues of several semi-analytical models (SAM) are available in the public database of the simulation. In this paper we study several SAMs (Bertone, De Lucia & Thomas 2007, Bower et al. 2006, De Lucia & Blaizot 2007, Guo et al. 2011, Font et al. 2008). In the models of Bertone, De Lucia & Thomas 2007, De Lucia & Blaizot 2007 and Guo et al. 2011 (BDLT07, DLB07 and G11 respectively hereafter), developed at the Max-Planck-Institute for Astrophysics (MPA) in Garching<sup>1</sup>, the galaxies are placed and evolved in the subhaloes according to their properties and their merger trees (Springel et al. 2005, Croton et al. 2006, De Lucia & Blaizot 2007). In the case of Bower et al. 2006 and Font et al. 2008 models (B06 and F08 hereafter), developed at the Institute for Computational Cosmology in Durham<sup>2</sup>, the merger trees

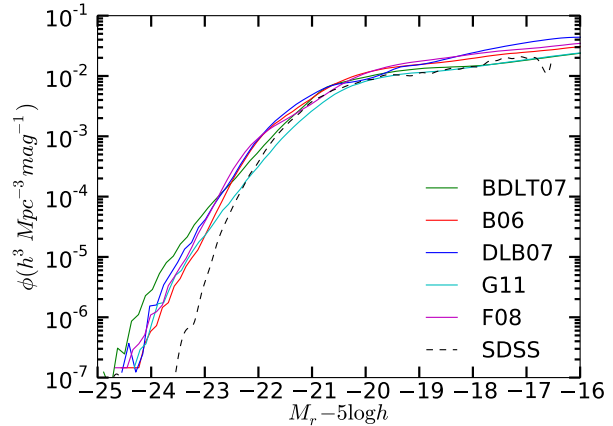


**Figure 2.** Luminosity Function of SAMs compared to the SDSS DR2 data (Blanton et al. 2005). Solid lines represent the different SAMs, and the dashed line shows the Luminosity Function from SDSS (Blanton et al. 2005).

are constructed using the *Dhaloes*, a different definition of halo consisting in groups of subhaloes (Helly et al. 2003). In most of the cases, the Dhaloes consist in the set of subhaloes of the same FOF, but in some cases (if the subhalo is outside twice the half mass radius of the parent halo or the subhalo has retained 75% of the mass it had at the last output time where it was an independent halo) these sets are divided in different Dhaloes (see Merson et al. 2013, Harker et al. 2006). Then the evolution of the latter models is related to halo (Dhalo) evolution, while the first models are associated to subhaloes. For this reason, the relation between Durham galaxies and subhaloes has not been studied.

In Fig. 2 we compare the luminosity function of all the SAMs studied with the luminosity function of SDSS DR2 (Blanton et al. 2005). To make coherent comparisons, we have used the luminosities in SDSS *r* filter of galaxies including dust extinction of the SAMs. In the case of DLB07, we used the Johnson *r* filter, and we applied a correction of  $-0.21$  to obtain the SDSS filter (see Fukugita et al. 1995). We applied a factor of  $5 \log h$ , with  $h = 0.73$ , in the MPA models, since this factor was not included in the database. In this Figure we can see an evident excess of bright galaxies in all the models. There is also a slight excess of galaxies in the faint end in the models DLB07, B06 and F08. This will produce visible consequences for Fig. 5, as explained in §3.1. However, Bernardi et al. (2013) studied different algorithms to obtain galaxy magnitudes and argued that the luminosity function from Blanton et al. (2003) in *r* band is probably underestimated for galaxies brighter than  $M_r < -22$ , so these differences do not necessarily reflect problems for the SAMs. These results are in agreement with Contreras et al. 2013, where they present a deeper comparison of the different semi-analytical models of the Millennium Simulation. Contreras et al. (2013) studied how much the clustering and HOD of these semi-analytical models depend on stellar mass, cold gas mass and star formation rate.

<sup>1</sup> <http://gavo.mpa-garching.mpg.de/MyMillennium/>

<sup>2</sup> <http://galaxy-catalogue.dur.ac.uk:8080/MyMillennium/>

### 3 BIAS AND HOD

In this section we present our measurements of halo, subhalo and galaxy bias needed for the different reconstructions of bias. We estimate the 2-Point Correlation Function (2PCF) using density pixels and the expression

$$\xi(r_{12}) = \langle \delta(r_1)\delta(r_2) \rangle, \quad (1)$$

where  $\delta(r)$  refers to the density fluctuation defined by  $\delta(r) = \rho(r)/\bar{\rho} - 1$  in pixels. From that, we measure the bias using the local bias model (Fry & Gaztañaga 1993):

$$b(r) = \sqrt{\frac{\xi_g(r)}{\xi_m(r)}} \quad (2)$$

where  $\xi_g(r)$  corresponds to the 2PCF of the studied object (haloes, subhaloes or galaxies),  $b(r)$  is the bias factor, and  $\xi_m(r)$  is the 2PCF of the dark matter field. As we assume  $b(r)$  to be constant at large scales, where  $\delta \ll 1$ , we define the mean value by fitting  $b(r)$  to a constant in the scale range  $20 h^{-1} \text{ Mpc} < r < 30 h^{-1} \text{ Mpc}$ . Although theoretically the bias may not be in the linear regime for these scales, we have checked that it behaves as a constant, so our fit can be assumed as valid. Moreover, the size of the Millennium Simulation does not allow us to go to larger distances with precision. The errors are measured with a Jack-Knife method (Norberg et al. 2009) of this measurement of  $b$ , using 64 cubic subsamples. The errors are taken from the standard deviation of these subsamples. The distribution of these subsamples is close to a gaussian, and the errors obtained from the percentiles are very similar to those from the standard deviation.

#### 3.1 Bias

In Fig. 3 we present the halo (top), main halo (middle) and subhalo (bottom) bias as a function of mass. We will refer to them as  $b_h(M)$ ,  $b_{mh}(M)$  and  $b_{sh}(M)$  and we compare the results with some analytical models. Using the mass function developed by Press & Schechter (1974) assuming the spherical collapse model, Mo & White (1996) derived the following expression for the halo bias:

$$b(\nu) = 1 + \frac{\nu^2 - 1}{\delta_c}, \quad (3)$$

where  $\delta_c = 1.868$  is the linear density of collapse and  $\nu = \delta_c/\sigma(M)$ , where  $\sigma(M)$  is the linear rms mass fluctuation in spheres of radius  $r = (3M/4\pi\bar{\rho})^{1/3}$ . Sheth, Mo & Tormen (2001) (SMT 2001) generalized and improved the expression using an ellipsoidal collapse model and they obtained the result:

$$b(\nu) = 1 + \frac{1}{\sqrt{a}\delta_c} \sqrt{a(av^2) + \sqrt{ab}(av^2)^{1-c}} - \frac{(av^2)^c}{(av^2)^c + b(1-c)(1-c/2)}, \quad (4)$$

with the parameters  $a = 0.707$ ,  $b = 0.5$  and  $c = 0.6$  tuned to work in N-body simulations. Finally, Tinker et al. (2010) presented a more flexible expression:

$$b(\nu) = 1 - A \frac{\nu^a}{\nu^a + \delta_c^a} + B\nu^b + C\nu^c. \quad (5)$$

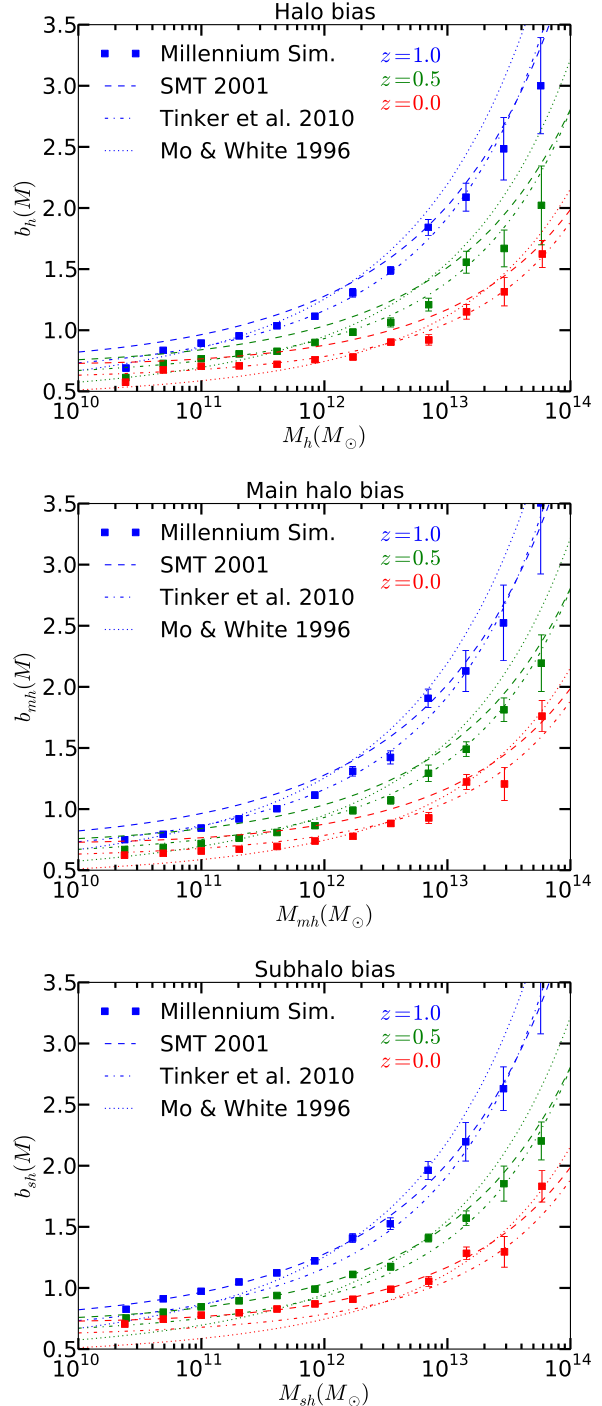


**Figure 3.** Halo (top), main halo (medium) and subhalo (bottom) bias as a function of mass at 3 different redshifts compared to theoretical expressions. The squares show the values of bias from the Millennium Simulation. Dashed lines show the analytic expression from Sheth, Mo and Tormen (2001) (equation (3)), dashed-dotted lines correspond to the Tinker et al. (2010) model, shown in equation (5), and dotted lines are the analytic expressions from Mo & White (1996), as in equation (4). Each colour represents a different redshift, as specified.

The values of the parameters of this expression used in our comparisons correspond to the values shown in Table 2 of Tinker et al. (2010) with  $\Delta = 200$ .

First of all, we can see that the SMT 2001 expression from equation (3) tends to overpredict  $b_h(M)$  and  $b_{mh}(M)$ , especially at low masses, but the agreement with  $b_{sh}(M)$  is remarkable. It is important to mention that subhaloes, as they are less massive than their haloes, present a higher bias for the same mass than the halos (and main halos). We can see a difference in the high mass region between haloes and main haloes due to the same effect, since for a given halo, the mass of the main halo is reduced (and then shifted to a lower mass) due to the SUBFIND unbinding process. On the other hand, the Mo & White (1996) equation (4) tends to produce an overprediction at high masses and an underprediction at low masses for all the cases. One possible reason for this is that Mo & White (1996) assume the Press-Schechter mass function, but this mass function fails to reproduce the halo mass function in simulations (Gross et al. 1998, Governato et al. 1999, Lee & Shandarin 1999, Sheth & Tormen 1999, Jenkins et al. 2001). Finally, the agreement of the Tinker et al. (2010) expression with  $b_h(M)$  and  $b_{mh}(M)$  is remarkable, while it underpredicts  $b_{sh}(M)$ , especially at low masses.

In Fig. 4 we show galaxy bias as a function of luminosity,  $b_g(L)$ , for these SAMs. The first 5 panels show  $b_g(L)$  in bins of luminosity for each of the studied SAMs, in the  $r$  band at 3 different redshifts, as specified. We also show in bottom right panel the comparison of these models with observations in the SDSS DR7 (Zehavi et al. 2011) using luminosity thresholds. To compute  $b_g(L)$  from the SDSS DR7 data, Zehavi et al. (2011) used a prediction of the dark matter correlation function from a  $\Lambda$ CDM cosmological model (Smith et al. 2003). Solid lines show the different SAMs, while the dashed-dotted line shows  $b_g(L)$  from Zehavi et al. (2011). As the cosmology assumed in Zehavi et al. (2011) is different than the one from Millennium, the dashed line corresponds to multiply the SDSS measurement by a factor  $0.8^2/0.9^2$ . This factor is an approximation of the difference in the amplitude of the dark matter field of both cosmologies if we assume that  $b_g(L)$  behaves as  $\sigma_8^2$ . Then, the dashed line shows an approximation of  $b_g(L)$  of the SDSS galaxies normalized by the Millennium cosmology.

First of all, we can see that  $b_g(L)$  increases with  $z$ , while the dependence on luminosity is not so strong in some models (BDLT07, DLB07 and G11), although the brightest galaxies show higher clustering amplitude. From the last panel, however, we observe discrepancies for all the models with observations from SDSS DR7 presented in Zehavi et al. (2011). We must mention the strong agreement between F08 and B06 models in the brightest galaxies. In general, the predicted  $b_g(L)$  is lower than in the observations for the brightest, and the shape of  $b_g(L)$  steepens only for the brightest galaxies in the SAMs, showing a shift with respect to the SDSS DR7 data. This shift depends strongly on the different cosmologies adopted between the SDSS analysis and the Millennium Simulation. As the value of  $\sigma_8$  is higher in the Millennium Simulation, their galaxy clustering is underpredicted due to the lower clustering of the dark matter of the simulation. The dashed line shows the com-

parison between the models and SDSS assuming the same dark matter field cosmology parameter  $\sigma_8$ . Here we can see that the agreement is good in the brightest galaxies, but the models disagree in the faintest region. From this panel, we can say that the agreement on  $b_g(L)$  between the models and the observations is strongly dependent on the cosmologies that we assume, but anyway the shape of  $b_g(L)$  of the models is different than that of SDSS data.

### 3.2 Subhalo Abundance Matching

To make our comparison wider, we also compare the SDSS DR7 measurements with some subhalo abundance matching (SHAM) methods. The results are shown in Fig. 5. We have constructed two galaxy catalogues by distributing the B06 galaxies into subhaloes using two different SHAM methods. The red solid line,  $SHAM_{mass}$ , corresponds to populating the subhaloes with galaxy luminosities assuming a monotonic relation between galaxy luminosity,  $M_r$ , and subhalo mass at present. However, when subhaloes are accreted by larger haloes, they lose an important fraction of their mass due to tidal stripping, and the fraction is larger for subhaloes which are closer to the centre (Muldrew et al. 2011). For this reason, subhalo mass can be a bad tracer of galaxy clustering. But the  $v_{max}$  depends on the central part of the subhalo, so only when the disruption of the subhalo affects most of the subhalo will the  $v_{max}$  be distorted (Knebe et al. 2011, Muldrew et al. 2011). Then,  $v_{max}$  retains more information about the past of the subhalo, when the galaxy was formed, than mass. For this reason, for the dotted line,  $SHAM_{vmax}$ , we distribute the galaxies according to a monotonic relation between  $M_r$  and subhalo  $v_{max}$  at present. No scatter has been applied to these matching processes. The same SHAM methods have been applied to a galaxy catalogue with the luminosity function of Blanton et al. (2005) (see dashed line from Fig. 2), constructed only for the purpose of this comparison, and the results are represented by the blue lines. We can see that the shape of  $b_g(L)$  in the SHAM galaxies is more similar to SDSS than SAMs, but the amplitude is still too small. One possible reason for this amplitude is the fact that we used the present properties of subhalo bias instead of taking into account subhalo evolution. Properties as  $v_{max}$  at the time of accretion or the maximum  $v_{max}$  ever for the subhaloes are better properties to fit galaxy clustering (Conroy, Wechsler & Kravtsov 2006, Simha et al. 2010, Reddick et al. 2012, Hearin et al. 2012). Scatter is also needed to fit galaxy clustering to observations (Trujillo-Gomez et al. 2011, Reddick et al. 2012, Hearin et al. 2012). On the other hand, the Millennium Simulation uses a different cosmology than the one adopted in the SDSS analysis. In particular, it assumes  $\sigma_8 = 0.9$ , which is a larger value than the one assumed in Zehavi et al. (2011). This produces an underestimation of the clustering of subhaloes, and consequently of these SHAM galaxies. A correction of the cosmology fixes an important part of the offset, as we see in the dashed black line, where we show the amplitude of the SDSS measurements corrected by a factor  $\sigma_8^2$  with respect to the Millennium cosmology, as in the lower right panel of Fig. 4.

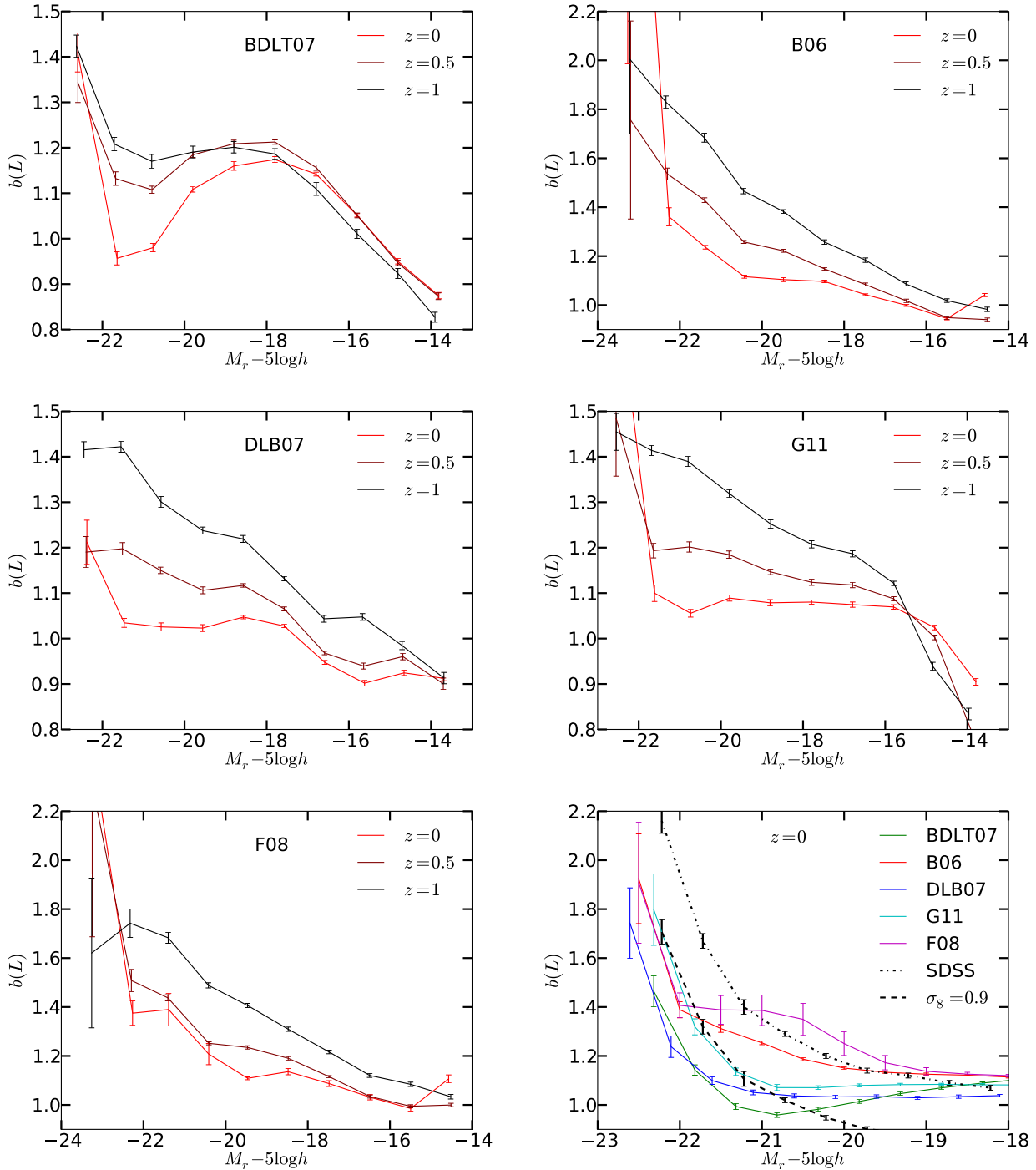


**Figure 4.** Luminosity dependence (in absolute  $r$  band magnitude) of galaxy bias for 5 SAMs and comparison with observations (bottom-right panel). The first 5 panels correspond to  $b_g(L)$  at  $z = 0, 0.5, 1$  for each SAM as labelled in magnitude bins. In the bottom right panel,  $b_g(L)$  of all the SAMs at  $z = 0$  are compared to  $b_g(L)$  from SDSS DR7 (Zehavi et al. 2011) in magnitude thresholds instead of bins. Solid lines represent the Millennium catalogues. The black dashed-dotted line corresponds to the SDSS DR7 data. The black dashed line shows a correction of  $0.8^2/0.9^2$  to approximate the amplitude of  $b_g(L)$  from SDSS if the 2PCF were normalized to a cosmology of  $\sigma_8 = 0.9$  instead of  $\sigma_8 = 0.8$ .

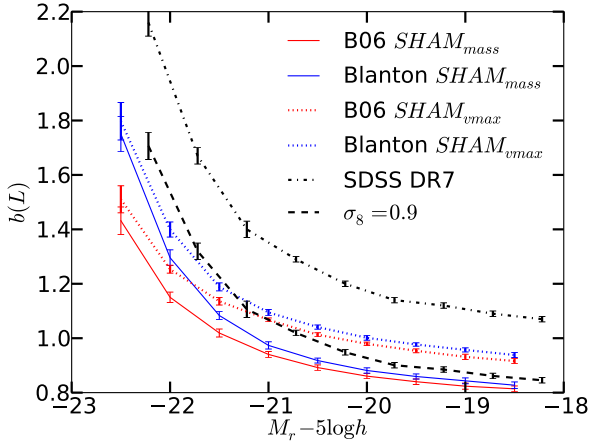


**Figure 5.** Luminosity dependence of galaxy bias for samples obtained applying simple SHAM prescriptions, compared to observations. The black dashed-dotted line corresponds to the SDSS DR7 data from Zehavi et al. (2011). The black dashed line correspond to the same  $\sigma_8$  correction than in the lower right panel of Fig. 4. The galaxies of the red lines correspond to distributing the B06 galaxies in subhaloes assuming a monotonic relation between the r-band luminosity and subhalo mass (solid lines) or  $v_{max}$  (dotted lines). The blue lines correspond to distribute galaxies with the luminosity function of SDSS from Blanton et al. 2005 into subhaloes assuming a monotonic relation between the r-band luminosity of the galaxies and the subhalo mass (dashed lines) or  $v_{max}$  (dotted lines).

Nevertheless, we can see important differences between the different catalogues. First of all, we can see that  $SHAM_{vmax}$  galaxies show higher  $b_g(L)$  than  $SHAM_{mass}$  in both cases. This reflects the fact that subhalo  $v_{max}$  is better related to clustering than subhalos mass (Reddick et al. 2012, Wake et al. 2012). On the other hand, we observe that for each SHAM method  $b_g(L)$  is slightly lower for B06 SHAM than for Blanton SHAM. This is common for any SAM used, although only the B06 SHAM is shown in Fig. 5. As the only difference between the Blanton catalogue and the SAM catalogue before applying the matching process is the Luminosity Function of the galaxies, we can argue that the difference of  $b_g(L)$  between these SHAM catalogues is due to this difference in the Luminosity Function (Fig. 2). In particular, we can see from Fig. 5 that B06 SHAM shows a shift to the brightest galaxies with respect to the Blanton SHAM. This shift is directly related to the excess of bright galaxies of the models because, as SHAM methods relate monotonically the luminosity of galaxies and the properties of the subhaloes, the galaxies with a given luminosity are hosted in smaller subhaloes (lower mass or  $v_{max}$ ) if there are more galaxies with a higher luminosity. This excess, then, causes a shift of the galaxies to lower subhalo masses (or  $v_{max}$ ). As the excess of bright galaxies is common for all the SAMs, it is no surprise that this shift appear in all the SAM SHAM catalogues.

### 3.3 HOD

SAMs of galaxy formation are not based on the halo model and hence they do not use the HOD prescription to populate galaxies into haloes. But effectively the models produce an HOD as an output, and we can study the occupation of galaxies in haloes or subhaloes and compare the mass dependence of the different populations. For each galaxy catalogue, we calculate the HOD by counting the galaxies per halo as a function of the halo mass. For the reconstructions of  $b_g(L)$  in §4, we will assume the HOD to be only dependent of halo (or subhalo) mass. We also analyse the luminosity dependence of these HODs. These distributions are shown in Fig. 6, where the HOD of some models are compared to the inferences from SDSS DR7 (Zehavi et al. 2011). Zehavi et al. (2011) inferred the HOD measurements from the clustering of different samples of galaxies assuming that the clustering of galaxies can be expressed in terms of the probability distribution that a halo of a given virial mass  $M_h$  hosts  $N$  galaxies of a given type. In this calculation they assume a  $\Lambda$ CDM cosmology with  $\Omega_m = 0.25$ ,  $\Omega_b = 0.045$ ,  $\sigma_8 = 0.8$ ,  $H_0 = 70 \text{ km s}^{-1} \text{ Mpc}^{-1}$  and  $n_s = 0.95$ . Dashed lines in Fig. 6 show the best fit of the HODs of the SDSS DR7 presented in Zehavi et al. (2011) using the equation:

$$\langle N(M_h) \rangle = \frac{1}{2} \left[ 1 + \operatorname{erf} \left( \frac{\log M_h - \log M_0}{\sigma_{\log M}} \right) \right] \left[ 1 + \left( \frac{M_h - M_0}{M'_1} \right)^\alpha \right], \quad (6)$$

where  $M_{min}$ ,  $\sigma_{\log M}$ ,  $M_0$ ,  $M'_1$  and  $\alpha$  are parameters to be fitted. The SAM measurements are shown by solid lines and each colour corresponds to a different threshold in magnitude,  $M_r$ . The top and middle panels show the HOD of four SAMs of the simulation (the prediction of the missing model, DLB07, is very similar to BDLT07), while the bottom panels show the HOD of the galaxy catalogues resulting from populating subhaloes applying  $SHAM_{mass}$  with G11 (left) and B06 (right) galaxies. The values of the HOD of the SAMs using the main haloes instead of the FOF groups, although it is not shown, is pretty similar. Given the fact that the main haloes have always lower mass than their respective FOF halo (since the difference with respect to the FOF is due to the application of the unbinding processes for dark matter particles),  $N(M_{mh})$  always has to be higher than  $N(M_h)$  for a given mass if the slope of the HOD is positive, as it is. At high masses, we note that although the original SAMs tend to have a higher population, the agreement with observations is remarkable, and excellent in the particular case of G11 model. At low masses, the level of agreement is model dependent, but the change of slope at  $\langle N_g(M_h) \rangle \approx 1$  tends to be softer in the SAMs than in the SDSS DR7 measurements.

On the other hand, in the case of the  $SHAM_{mass}$  catalogues we can see large discrepancies with observations. We can see a lack of faint galaxies at high masses, and an excess of galaxies at low masses, with the opposite trend for the brightest galaxies. We observe that, especially at low masses, the main contribution to the HOD for a given mass comes from only one magnitude bin. In some sense, the relation between the luminosity of the galaxy and the mass of the host halo is stronger than in the observations, since

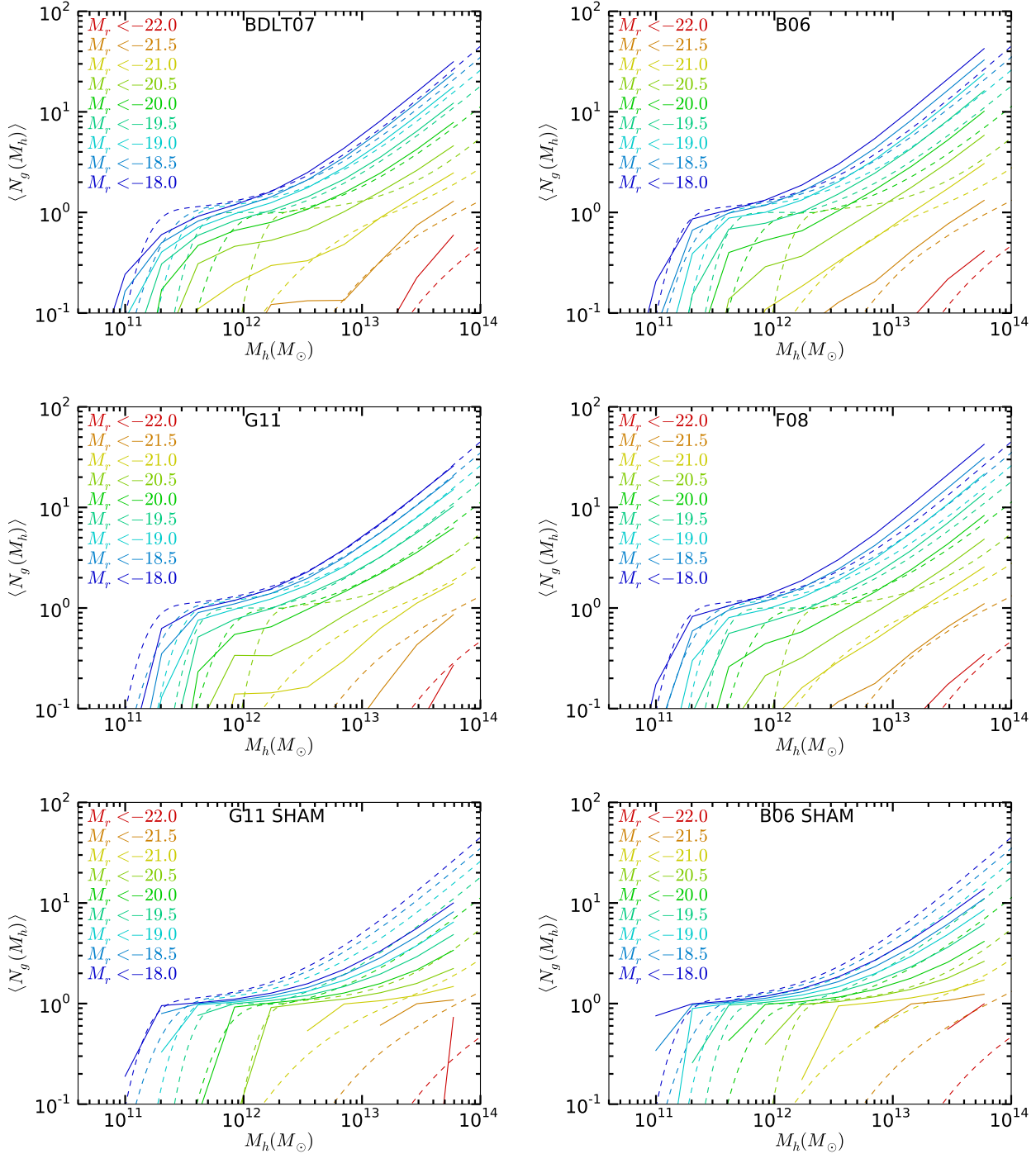


**Figure 6.** HOD of galaxies for the different SAMs (solid lines) compared to the HOD found by Zehavi et al. (2011) from the SDSS DR7 data (dashed lines). Top panels correspond to the BDLT07 (left) and B06 (right) models, middle panels show G11 (left) and F08 (right) models, and bottom panels correspond to *SHAM*<sub>mass</sub> catalogues using galaxies from G11 (left) and B06 (right) models. Each colour corresponds to a luminosity threshold in units of  $M_r - 5 \log h$  as specified.

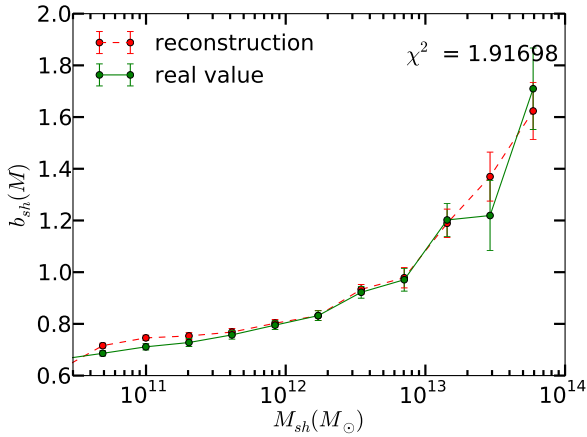


**Figure 7.** Reconstruction of  $b_{sh}(M)$  from  $b_h(M)$  at  $z = 0$ . The dashed red line corresponds to the reconstructed  $b_{sh}(M)$ , while green solid line represents the true value of  $b_{sh}(M_h)$ .

galaxies of a given luminosity tend to be in a fixed halo mass. This is due to the relation between the subhalo mass and its host halo mass. As the  $SHAM_{mass}$  galaxies assume a monotonic relation between luminosity and  $M_{sh}$ , the luminosity thresholds of the  $SHAM_{mass}$  galaxies can be seen as a direct translation of thresholds in  $M_{sh}$  of the subhaloes. Then, bottom panels of Fig. 6 show directly the  $M_h$  dependency of the  $M_{sh}$  distribution of subhaloes. The behaviour in the bottom panels at low halo masses shows that the luminosity (and then  $M_{sh}$ ) is strongly related to  $M_h$ , since for each  $M_h$  we have a fixed  $M_r$  ( $M_{sh}$ ). Then, we see that the  $M_h$  dependence is stronger for  $M_{sh}$  than for the  $M_r$  of SAMs and SDSS. For this reason, we can argue that  $M_h$  contains more information about  $M_{sh}$  than about  $M_r$ , and so the reconstruction of  $b_{sh}(M)$  from  $b_h(M)$  can be more precise than the one of  $b_g(L)$  from  $b_h(M)$  (see §4). Finally, comparing the bottom panels with the HODs of the original SAMs together with Fig. 4 we can confirm that there is not a monotonic relation between  $M_{sh}$  and  $M_r$  in the SAMs of the Millennium Simulation. The distortion of this relation can cause problems when trying to reproduce  $b_g(L)$  from  $b_{sh}$ , as we show in §4.

#### 4 GALAXY BIAS RECONSTRUCTIONS

The HOD model assumes that the galaxy population of haloes depends only on the halo mass. If this is true, then it is possible to predict measurements of galaxies such as  $b_g(L)$  from the measurements of  $b_h(M)$  once we know the mass of the haloes and the HOD of galaxies in haloes. In this section, we assume that the populations of galaxies and subhaloes depend only on the mass of their host objects (subhaloes, main haloes or haloes), and we use the following formula (Scoccimarro et al. 2001, Cooray et al. 2004, Wechsler et al. 2006, Coupon et al. 2011) to make the reconstructions of

$b_g(L)$  and  $b_{sh}(M)$ :

$$b_\beta(z) = \int dM b_\alpha(M, z) n_\alpha(M, z) \frac{N_{\beta\alpha}(M)}{n_\beta(z)} \quad (7)$$

where  $\beta$  refers to the object to which we predict the bias (galaxies or subhaloes) and  $\alpha$  is the object from which we use the bias (subhaloes, main haloes or haloes).  $n(z)$  corresponds to the number density of the specified object and  $N_{\beta\alpha}(M)$  is the mean number of  $\beta$  objects per  $\alpha$  object of mass  $M$ , so the HOD of  $\beta$  in  $\alpha$ . In other words, we are assuming that the HOD not only works for galaxies in haloes, but also for other objects and hosts. These other assumptions are not based on the halo model, but can be used as a measure of the dependence of galaxy and subhalo clustering on the mass of different objects such as FOF groups, spherical haloes or subhaloes. As we use a range in mass in  $\alpha$ , the  $\beta$  sample is restricted to those objects which are inside the considered  $\alpha$  objects, excluding those which are outside the range of  $N_{\beta\alpha}(M)$ . The error of the reconstruction is obtained by calculating the Jack-Knife error of the reconstruction using 64 cubic subsamples. Finally, in all the reconstructions  $\chi^2$  is calculated according to the formula:

$$\chi^2 = \frac{1}{N} \sum_i^N \frac{M_i - R_i}{\sigma_{M,i}^2 + \sigma_{R,i}^2}, \quad (8)$$

where  $N$  is the number of data points,  $M$  and  $R$  are the measured and reconstructed points respectively, and  $\sigma_{M,i}$  and  $\sigma_{R,i}$  are the respective errors of  $M$  and  $R$ .

Fig. 7 shows the reconstruction of  $b_{sh}(M)$  from  $b_h(M)$  (top panel in Fig. 3). There is a good qualitative agreement, meaning that we can assume that  $N_{sh,h}(M)$  depends strongly enough on  $M_h$  to consider subhaloes good tracers of halo clustering. Nevertheless, note that the  $\chi^2$  fit is too high, the reconstruction tends to slightly overestimate the real value of  $b_{sh}(M)$  at low masses.

For the reconstructions of  $b_g(L)$ , we will focus on the G11 and B06 models in  $M_r$  as representatives of MPA and Durham models to analyse the reconstructions. Although the SAMs have clear differences in the luminosity dependence of  $b_g(L)$ , the results of the reconstructions of all the SAMs present similar behaviour and the same qualitative conclusions in G11 and B06. In all these reconstructions we have excluded all the galaxies in dark matter hosts (haloes, main haloes or subhaloes) with  $M > 8.6 \times 10^{13} M_\odot$  in order to avoid large errors. At high masses, the bias steepens, and there is also a lack of statistics, and because of this the errors of the reconstructions are too large if we include these masses. We understand that these errors are due to our statistical limitations of these high masses and do not allow us to obtain strong conclusions from low masses. Then, the exclusion of these masses in the reconstructions must be understood as a test of the HOD for all the masses below this threshold of  $M = 8.6 \times 10^{13} M_\odot$ . We do not study galaxies fainter than  $M_r < -14$  in order to avoid incompleteness effects.

Fig. 8 shows the reconstructions of  $b_g(L)$  from haloes of these two models at  $z = 0$  and 1. The reconstructions are shown in red, and they are compared to the real values,

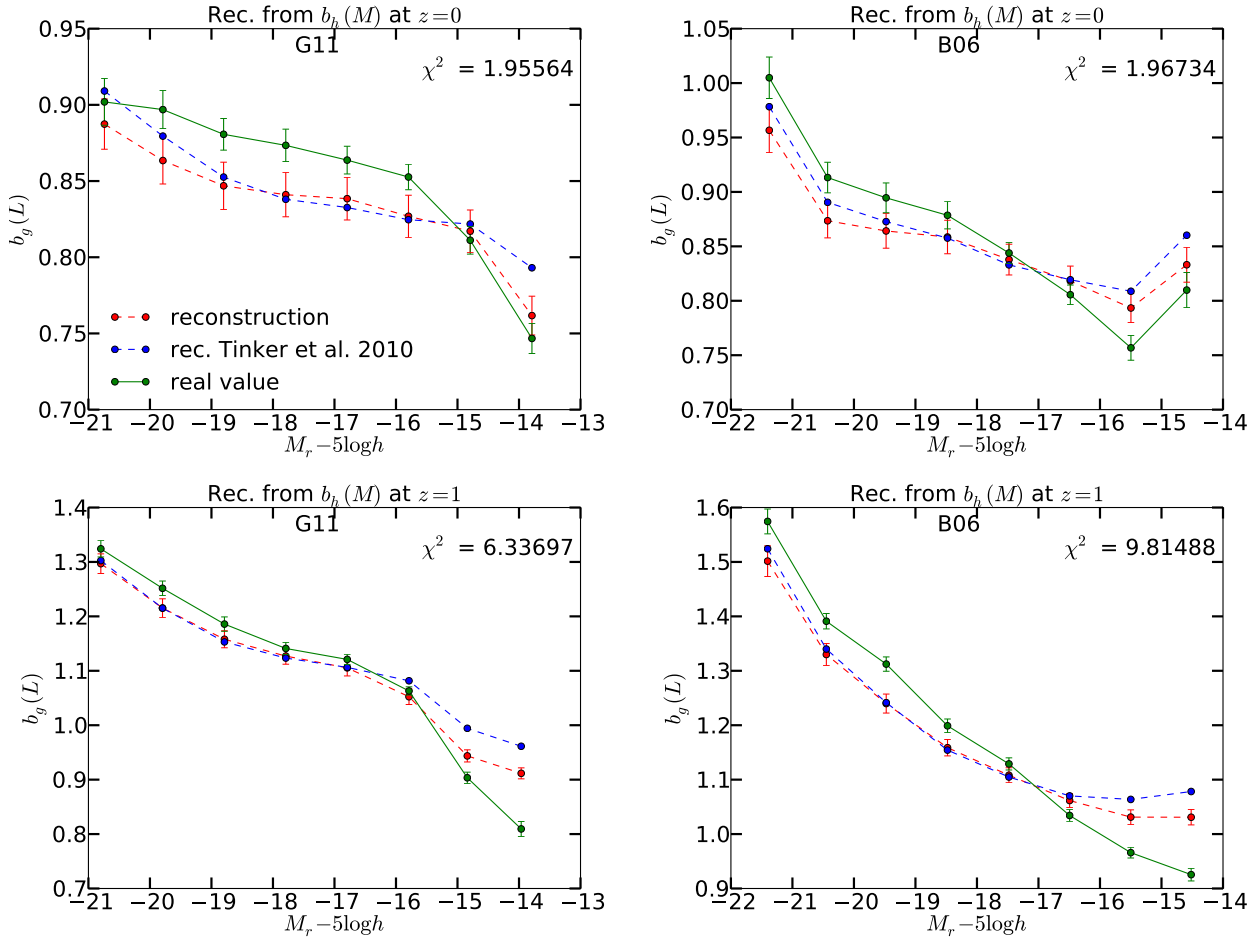


**Figure 8.** Reconstructions of  $b_g(L)$  from  $b_h(M)$  at  $z = 0$  and  $z = 1$ . The dashed red line corresponds to the predicted  $b_g(L)$ , while green solid line represents the real measured value of  $b_g(L)$ , and the dashed blue line corresponds to the reconstructions using the values of  $b_h(M)$  from the Tinker et al. (2010) model. Left panels corresponds to G11 model, while right panels show predictions for the B06. On top,  $z = 0$ . On bottom,  $z = 1$ .

in green. We also show in blue the reconstruction using the values of the Tinker et al. (2010) model for  $b_h(M)$  instead of the measurements of the simulation in order to compare the differences between modelling and measuring  $b_h(M)$  for the reconstruction. Top panels show  $z = 0$  and bottom panels are at  $z = 1$ . Finally, in the left panels we see the reconstructions of G11, and in the right panels we used the B06 model. In Fig. 9 we show the reconstructions of  $b_g(L)$  from  $b_{mh}(M)$  for the same SAMs and redshifts.

First of all, we can see that the reconstructions tend to be better at low redshift, but this is mainly due to the disagreement of the reconstructions at  $z = 1$  for the faintest galaxies. Secondly, the reconstructions using the Tinker et al. (2010) model are typically very close to the reconstructions from the measurements of  $b_h(M)$ . This might indicate that the volume of the simulation is large enough to calculate these reconstructions. If the Tinker et al. (2010) model is correct, then increasing the volume and statistics of the simulation would reduce the errors of the reconstruction, but the values should not change significantly. On the other

hand, the reconstructions from  $b_{mh}$  are different from using the Tinker et al. (2010) model at the level of  $1\sigma$ . This means that the Tinker et al. (2010) model is more consistent with the FOFs haloes than with the main haloes. Another important result independent of the SAMs and redshift is the fact that haloes predict better  $b_g(L)$  than main haloes. This means that the unbinding processes, somehow, loses information about the galaxy clustering. In some sense, the mass of the FOF groups are more directly related to the clustering of these regions than the mass restricted to the bound particles in spherical overdensities, maybe because the FOF groups include more environment of the overdensity. Finally, we can see the effect of the the reconstructions are flatter than the real values or, in other words, the reconstruction overpredicts  $b_g(L)$  for faint galaxies and underpredicts  $b_g(L)$  for bright galaxies. This is a constant effect in  $z$  and appears using  $b_h(M)$ ,  $b_{mh}(M)$  or  $b_{sh}(M)$  (see Fig. 10). This effect is analysed more in detail in §4.1.

However, the reconstructions from  $b_{sh}(M)$  do not work, as shown in Fig. 10 for the G11 model. In the left panel

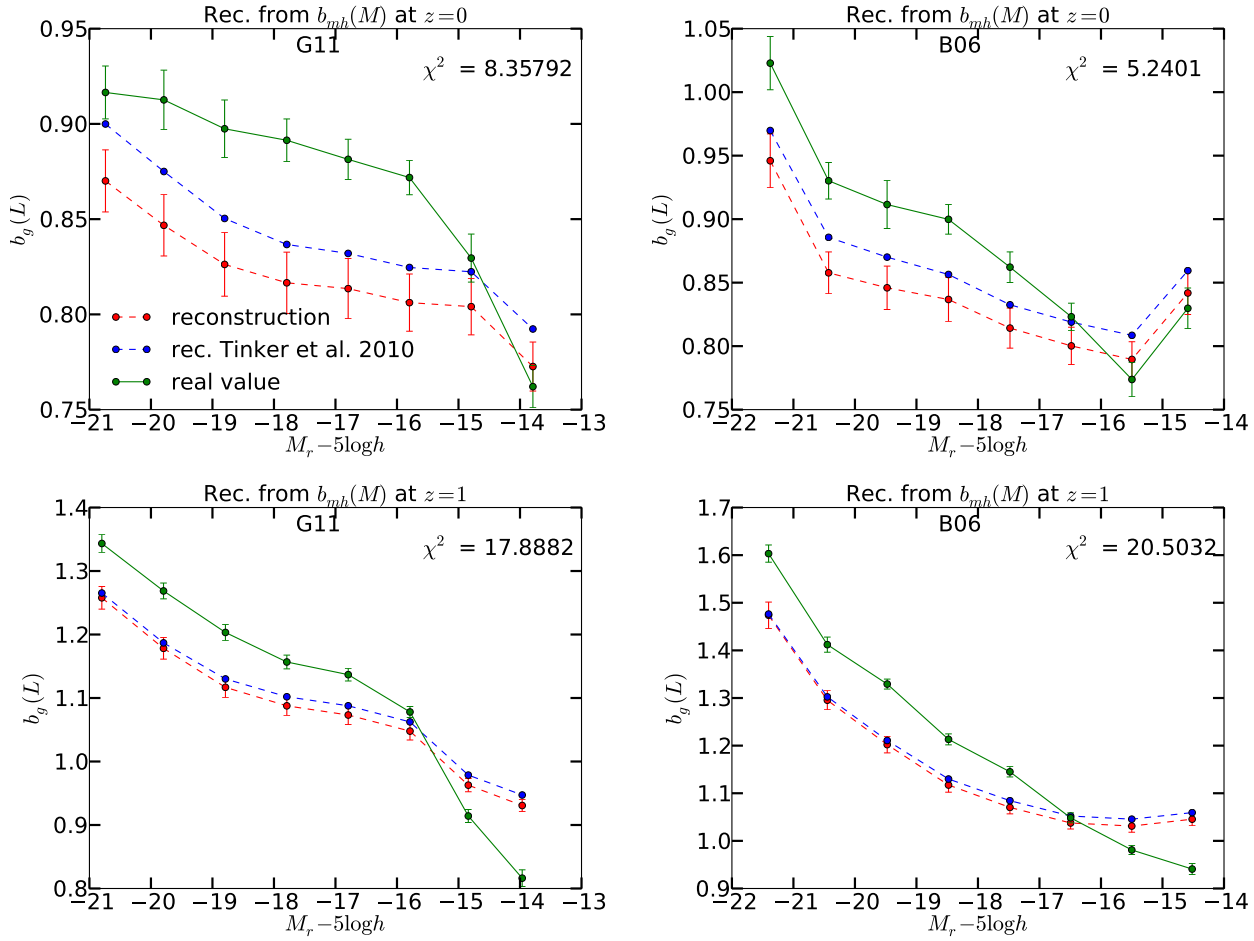


**Figure 9.** The same as in Fig. 8, but the reconstructions are obtained from  $b_{mh}(M)$  instead of  $b_h(M)$ .

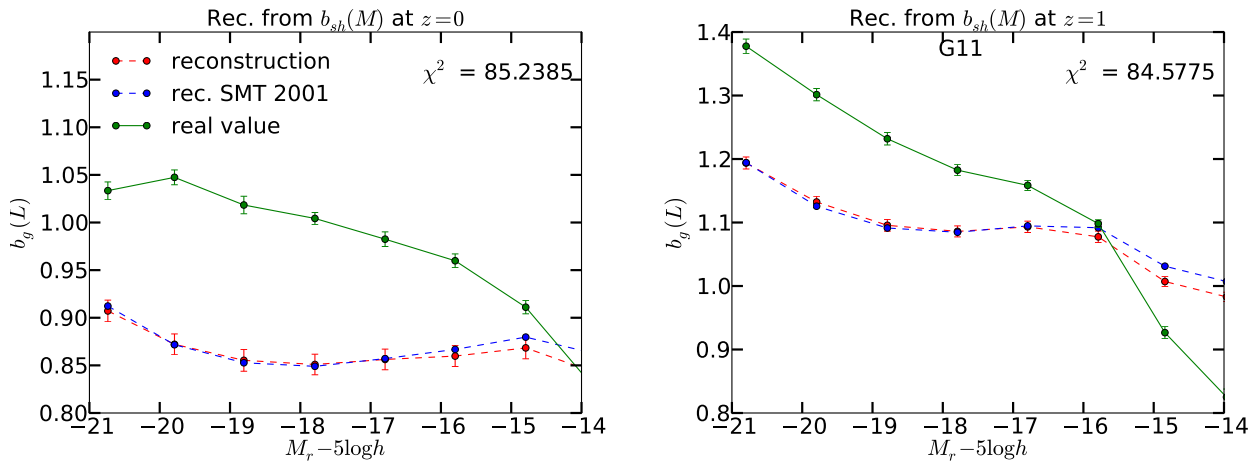


**Figure 10.** The same as in Figs. 8 and 9, but the reconstructions are obtained from  $b_{sh}(M)$  instead of  $b_h(M)$  or  $b_{mh}(M)$ . In blue, SMT 2001 model has been used for the values of  $b_{sh}(M)$  instead of Tinker et al. (2010), since  $b_{sh}(M)$  is shown to be closer to the SMT 2001 mass function from Fig. 3. Only the G11 model is shown, at  $z = 0$  (left) and  $z = 1$  (right).

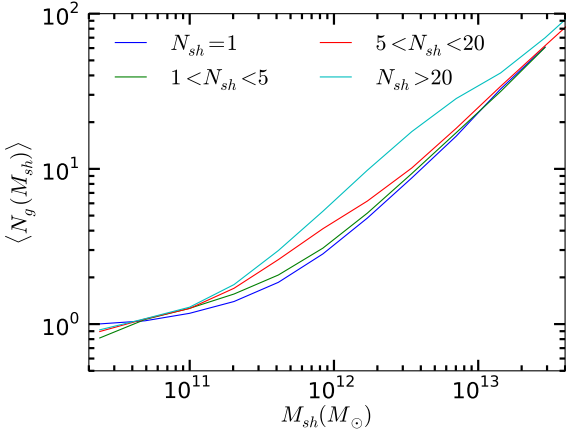


**Figure 11.** Occupation of galaxies in subhaloes as a function of their subhalo mass,  $\langle N_g(M_{sh}) \rangle$ , for the DLB07 model. Each colour represents only the galaxies in haloes with the corresponding number of subhaloes,  $N_{sh}$ .

$z = 0$  is shown, and  $z = 1$  is shown in the right panel. We do not show Durham SAMs, since the galaxies are linked to the Dhaloes but not to the subhaloes, as mentioned in §2. We can see that there is a large difference between the real values and the predicted ones, meaning that the mass of the subhaloes is not a good tracer of galaxy clustering. Also, the flattening effect is much stronger than the previous ones. Here we used the SMT 2001 model for  $b_{sh}(M)$  instead of Tinker et al. (2010), since this model is the closest to the measurement of  $b_{sh}(M)$  (see Fig. 3). The agreement between modelling and measuring  $b_{sh}(M)$  is very good.

#### 4.1 Subhalo population

In this section we divide the samples into subsamples depending on the amount of substructure in the host halo. The idea is to separate the haloes and their content depending on the amount of subhaloes inside the haloes,  $N_{sh}$ , to see if galaxies depend on their halo substructure. This is an indirect measurement of environment, since the amount of subhaloes in a halo depends on the merging history of the halo, which is related to the environmental abundance of haloes. First of all, we can see in Fig. 11 that the galaxy population depends on the amount of substructure in the host halo. The important result is that, for a given subhalo mass  $M_{sh}$ , the number of galaxies per subhalo depends on  $N_{sh}$ . Because of this, a separation of the sample of galaxies and subhaloes according to this factor can be important to make a good reconstruction of  $b_g(L)$ .

The difference is not only in the galaxy population but also in the clustering of subhaloes and galaxies. In Fig. 12 we can see  $b_h(M)$ ,  $b_{sh}(M)$  and  $b_g(L)$  separating the samples of haloes, subhaloes and galaxies according to the number of subhaloes in their host halo. In the case of  $b_h(M)$ , shown in the top left panel, different values of  $N_{sh}$  cover different ranges of mass. These are the regions where there are good halo statistics. We can see that there is a relation between

$N_{sh}$  and mass, such that the most massive haloes are the most occupied of subhaloes, and the smallest ones the least occupied. Apart from this, we can see that, given a fixed mass, there are no clear differences in halo clustering between haloes with different occupations. However, the cases of  $b_{sh}(M)$  and  $b_g(L)$  are completely different. Two conclusions can be obtained from Fig. 12 about galaxies and subhaloes: (1) for a fixed  $M_{sh}$  (at low masses at least) or  $L$ , the dependence of  $b$  on subhalo occupation,  $N_{sh}$ , is very strong, and (2) for a fixed  $N_{sh}$  there is not a strong dependence of  $b$  on  $M_{sh}$  or  $L$ . So, in some sense, the main information about the subhalo clustering does not reside in its mass, but in its host halo occupation, which is sensitive to the environment. Once we know this  $N_{sh}$ ,  $M_{sh}$  do not give substantial information about  $b_{sh}(M)$  or  $b_g(L)$ . This could be one reason for the disagreement of the reconstruction of  $b_g(L)$  from  $b_{sh}(M)$ , since we are merging subhaloes with different  $N_{sh}$  (and clustering) into the same mass bins, and this produces a distortion of the final bias reconstruction.

In order to go further into the effect produced by the occupation dependence, we have computed the reconstruction of  $b_g(L)$  for two samples separately. In Fig. 13 we show the reconstructions of  $b_g(L)$  for G11 galaxies from subhaloes in haloes with  $N_{sh} = 1$  (left) and for G11 galaxies from subhaloes in haloes with more than 1 subhalo (right) at  $z = 0$ . We must notice that the reconstructions in haloes with  $N_{sh} > 1$  and  $N_{sh} = 1$  separately work much better than using the whole sample of subhaloes. This means that  $b_g(L)$  is strongly constrained by  $N_{sh}$ . On the other hand, the reconstruction using the sample of haloes with  $N_{sh} > 1$  is better than the reconstruction in haloes with  $N_{sh} = 1$ . In this second case the flattening effect is also strong. This means that the HOD assumption does not work well for galaxies in haloes with  $N_{sh}(M_h) = 1$ , i.e. the smallest ones, since in these cases the main haloes and the subhaloes are the same object.

To understand the error in the reconstructions for the brightest and faintest galaxies, we measured  $b_g(L)$  in several narrow  $M_{sh}$  bins. Fig. 14 shows  $b_g(L)$  for galaxies in different  $M_{sh}$  bins. Each colour corresponds to a  $M_{sh}$  range. The lines show  $b_g(L)$  for galaxies in subhaloes with the respective host subhalo mass, and the horizontal coloured zones represent the measured ranges  $b_{sh}(M_{sh}) \pm 1\sigma$  of each  $M_{sh}$  bin (see bottom panel of Fig. 3). This figure, then, allow us to explain the reconstructions of galaxy bias, since to each galaxy of a given  $b_g(L, M_{sh})$  we associate a bias  $b_{sh}(M_{sh})$ . Then, the reconstruction works if the values of  $b_g(L, M_{sh})$  are close to  $b_{sh}(M_{sh})$ . In Fig. 14 we can see three different behaviours. At high masses,  $b_g(L, M_{sh})$  is close to  $b_{sh}(M_{sh})$ , since the solid lines tend to be close or inside their coloured zones. For the intermediate masses (between  $10^{11}$  and  $10^{13} h^{-1} M_\odot$ )  $b_g(L, M_{sh})$  tends to be shifted to a higher bias respect to  $b_{sh}(M_{sh})$ . Finally, and the most important effect, in the low mass regions of  $M_{sh}$  there is a strong disagreement between  $b_g(L, M_{sh})$  and  $b_{sh}(M_{sh})$ . The bias of the brightest galaxies is much higher than the one in the subhaloes of the corresponding mass, and the faintest are much less clustered. So, in these low masses, the galaxies are populated precisely in a way where the dimmest galaxies are in the less clustered

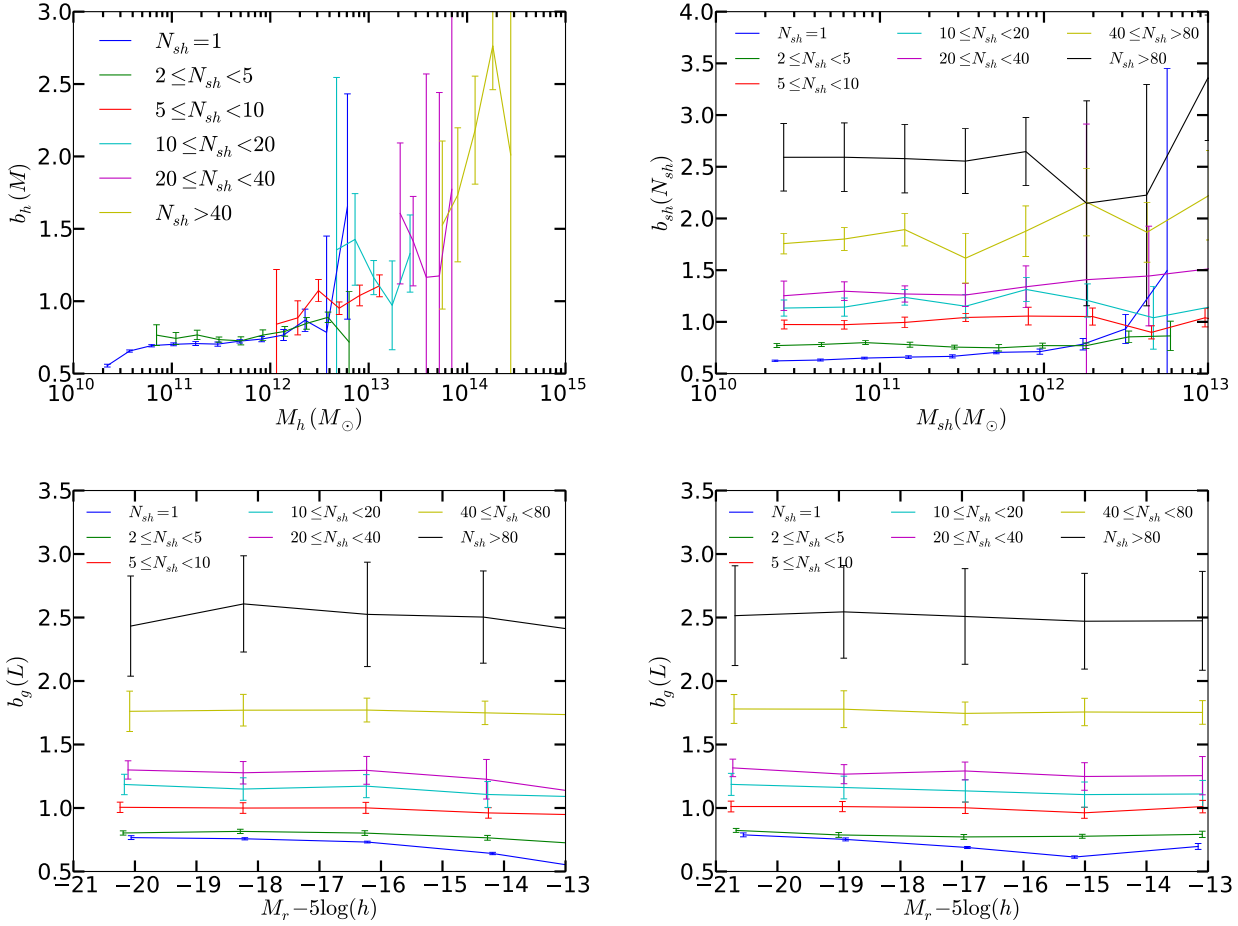


**Figure 12.** Top:  $b_h(M)$  (left) and  $b_{sh}(M)$  (right) for different samples according to their number of subhaloes  $N_{sh}$  inside. Bottom:  $b(L)$  for galaxies in haloes with different  $N_{sh}$  for G11 (left) and B06 (right) models. All the panels are at  $z = 0$ .

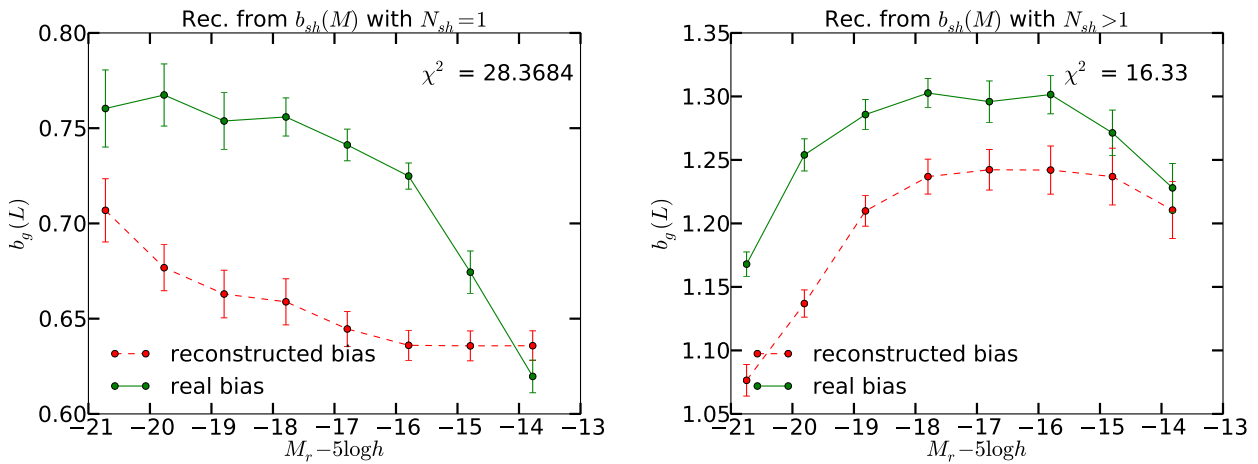


**Figure 13.** Reconstruction of  $b_g(L)$  from  $b_{sh}(M)$  in two different samples of the G11 model. The left panel shows the reconstruction of galaxies in haloes with  $N_{sh} = 1$ , and the right panel shows the prediction for galaxies in haloes with  $N_{sh} > 1$ . Both are at  $z = 0$ .

subhaloes, and the brightest galaxies in the most clustered ones for the same mass  $M_{sh}$ . This means, then, that the clustering of these galaxies is weakly dependent on subhalo mass. As the fraction of galaxies that are located in low mass subhaloes is large, this effect is very important in the final reconstructions of Fig. 10 and 13 (right panel). However, when we restrict the galaxies to haloes with more than one subhalo (Fig. 13, left panel), the effect of low masses becomes weaker, and the underprediction due to the effect of intermediate masses becomes visible.

On the other hand, as the distortion of the reconstructions is important in the low  $M_{sh}$  region, the exclusion of this region should improve our  $b_g(L)$  reconstruction from  $b_{sh}(M)$ . Fig. 15 shows this reconstruction using subhaloes with more than 60 particles (left) and with more than 300 particles (right). We can see that the exclusion of the smallest subhaloes improves substantially the reconstruction. We must notice also the changes that this exclusion makes on the shape of the real  $b_g(L)$ . We can see, in particular, that excluding the galaxies in small subhaloes increases the clustering for the dimmest galaxies but not the clustering of the brightest galaxies. This is a problem when trying to recover the luminosity dependence of galaxy clustering from observations, as in Fig. 4, as we will see in Fig. 18.

Finally, in Fig. 16 we show the same as in Fig. 14 but using haloes instead of subhaloes. So, the samples of galaxies are split according to the mass of the host halo, and the coloured regions correspond to the values of  $b_h(M) \pm 1\sigma$  of the corresponding mass bins (top panel of Fig. 3). Although we don't show the corresponding figure using main haloes, the result is very similar to Fig. 16. We note that, as in the case of the subhalo mass, there is no halo mass dependence of  $b_g(L)$  at low masses. As this also occurs with the main haloes and for all the SAMs, we can argue that this weakness of the HOD assumptions at low masses is independent of the definition of halo or subhalo used in the Millennium Simulation and could be intrinsic to dark matter haloes. As there are fewer haloes than subhaloes at low masses (see Fig. 1) and most of the galaxies reside in large haloes, the effect of this masses in the reconstruction of  $b_g(L)$  is smaller than in subhaloes, and this is the reason why the reconstructions work better. The case of the main haloes is very similar to the case of the haloes, but there are more galaxies residing in low mass main haloes than in low mass haloes, since the mass of the halo is always higher than the mass of the corresponding main halo. For this reason, the lowest masses in the reconstructions of  $b_g(L)$  from  $b_{mh}(M)$  are more important than in the reconstructions of  $b_g(L)$  from  $b_h(M)$ , and then the reconstructions from  $b_{mh}(M)$  are slightly worse than the reconstructions from  $b_h(M)$ .

In order to measure the effect of the small haloes in the reconstructions, in Fig. 17 we show the reconstruction of  $b_g(L)$  restricting the samples of galaxies according to the host halo mass thresholds of more than 60 particles (left) and 300 particles (right). As in the case of subhaloes from Fig. 15, the exclusion of the low mass regions improves the reconstruction, but distorts the luminosity dependence of  $b_g(L)$ . So, although the success of the reconstructions is different for the different dark matter objects used, the problems of

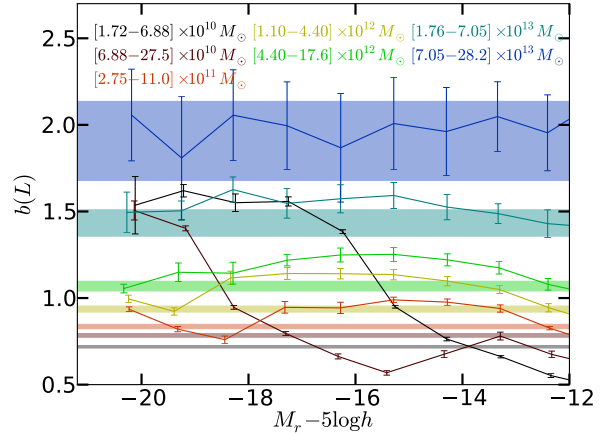


**Figure 14.**  $b_g(L)$  for different subhalo mass bins for G11 galaxies. Each colour corresponds to a subhalo mass bin as indicated. Solid lines represent galaxy bias with  $r$ -band luminosities of those galaxies in the subhaloes of the corresponding range in mass. The horizontal coloured zones refer to the ranges  $b_{sh}(M_{sh}) \pm 1\sigma$  of each  $M_{sh}$  bin.

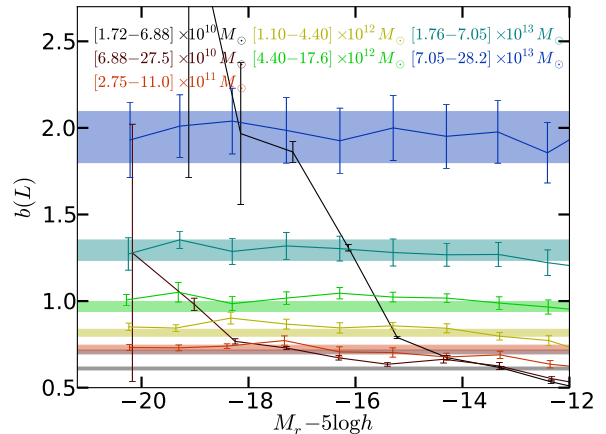


**Figure 16.** The same as Fig. 14 but using the mass bins and the bias of the host haloes instead of host subhaloes.

the HOD assumptions and luminosity dependences found at low masses in these different objects have been found to be the same.

Finally, in Fig. 18 we show  $b_g(L)$  of the G11 model restricted to galaxies in haloes of different mass thresholds, to explicitly see how much the luminosity dependence of galaxy bias changes by suppressing the galaxies in small haloes. We compare these samples with the SDSS DR7 data from Zehavi et al. (2011). We can see that excluding galaxies in haloes with  $M_h < 2.58 \times 10^{11} h^{-1} M_\odot$  does not affect the brightest galaxies. However, the faintest galaxies are strongly affected by the exclusion of these masses, and the range of luminosities affected increases with the  $M_h$  threshold. In general, for a fixed luminosity, satellite galaxies are more strongly clustered than centrals, since satellites have been merged

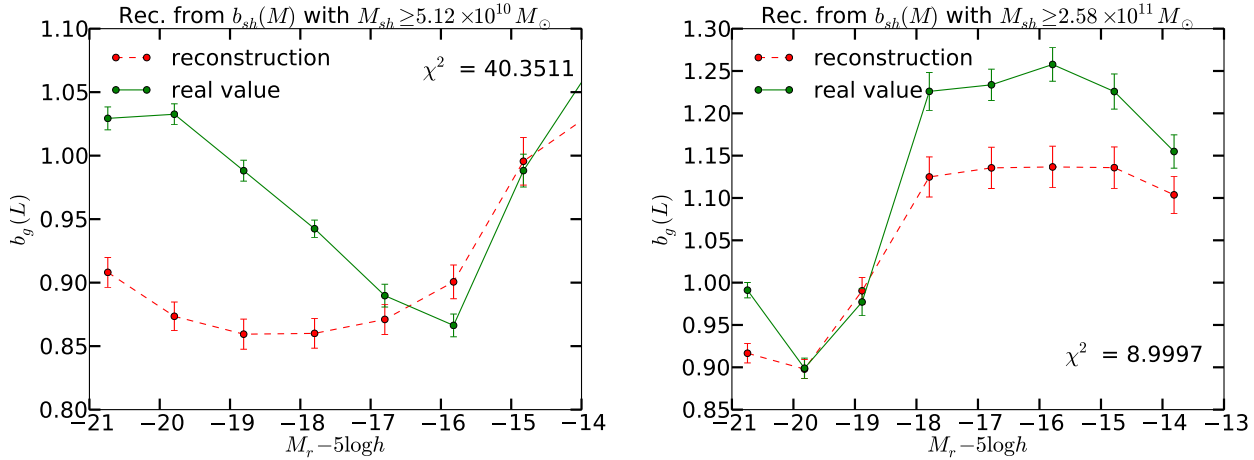


**Figure 15.**  $b_g(L)$  in  $r$  filter (solid green lines) and its reconstruction (dashed red lines) from  $b_{sh}(M)$  for different  $M_{sh}$  threshold cuts. In the left panel, only subhaloes with more than 60 particles ( $5.12 \times 10^{10} h^{-1} M_{\odot}$ ) are used. In the right panel, the samples are restricted to those subhaloes with more than 300 particles ( $2.58 \times 10^{11} h^{-1} M_{\odot}$ ).

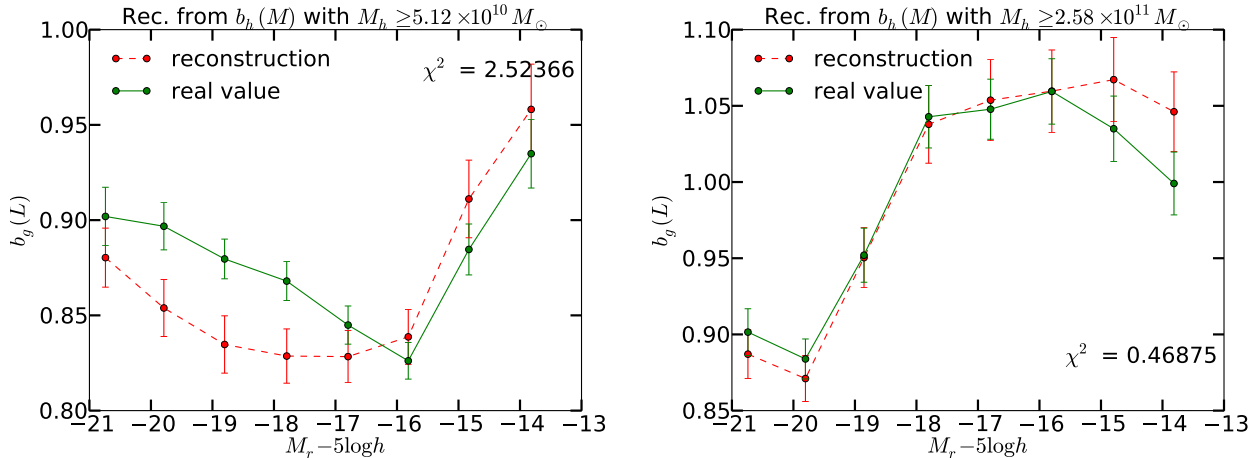


**Figure 17.** The same as in Fig. 15 but using haloes instead of subhaloes. In the left panel, only haloes with more than 60 particles ( $5.12 \times 10^{10} h^{-1} M_{\odot}$ ) are used. In the right panel, the samples are restricted to those haloes with more than 300 particles ( $2.58 \times 10^{11} h^{-1} M_{\odot}$ ).

to a larger structure, while faint central galaxies still reside in small haloes with weak clustering. When we exclude the smallest masses, we are mainly excluding dim central galaxies, and then for these luminosities the remaining satellites increase the measurement of  $b_g$ . For the dimmest galaxies, we exclude the satellite galaxies of these small haloes, and the clustering of the remaining galaxies increases even more. This is the effect we see in Fig. 18. We see that we cannot exclude the smallest haloes in order to reproduce SDSS clustering, so we can say that fixing the HOD assumptions by suppressing the galaxy populations of the smallest haloes is incompatible with reproducing galaxy clustering from observations.

## 5 SUMMARY AND DISCUSSION

We used the Millennium Simulation to study the clustering of galaxies as predicted by semi-analytical models (SAM) of galaxy formation and the dependence of clustering on luminosity in the SDSS  $r$  band filter. We have found discrepancies with respect to observations (Zehavi et al. 2011) that can be due in part to their excess of bright galaxies and in part due to the differences on the assumed cosmology for the analysis, in particular the difference in  $\sigma_8$ . Although the SAMs are not based on the HOD model, their populations agree with the observations of the HOD from the SDSS DR7 (Zehavi et al. 2011). We assumed the HOD model to reproduce galaxy bias from halo (FOF groups), main halo (gravitationally bound haloes) and subhalo bias as a function of mass, assuming that the population of galaxies only

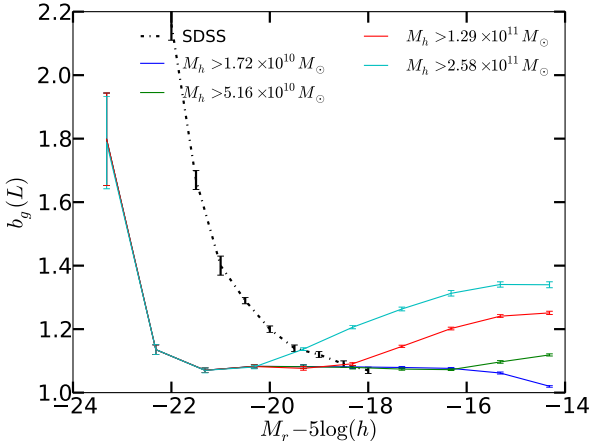


**Figure 18.**  $b_g(L)$  of the G11 model for galaxies in haloes larger than different mass thresholds (solid lines) compared to SDSS DR7 from Zehavi et al. (2011) (dashed).

depends on the mass of these objects. From our study we obtain the following results:

(i) The reconstructions do not provide a good  $\chi^2$  to simulations ( $\chi \gtrsim 2$ ), but the general trend is correct within  $\gtrsim 5\%$  accuracy.

(ii) FOF groups make better reconstructions of  $b_g(L)$  than the main haloes, which could be due to the fact that FOF groups include more information about the environment than the main haloes. Moreover, in almost all the cases, the reconstructions work better for higher redshifts, so the galaxy luminosity of the SAMs is less (sub)halo mass dependent when the halo mass has evolved due to processes such as merging and tidal stripping.

(iii)  $b_g(L)$  cannot be recovered from  $b_{sh}(M)$  in general, although higher redshift have better results. The luminosity dependence of the reconstructions of  $b_g(L)$  from subhaloes tend to be flatter than the real values. This indicates that the subhalo mass is not a good tracer of galaxies.

(iv) The clustering of subhaloes and galaxies depends strongly on the amount of substructure in their host haloes. For a fixed halo occupation (of subhaloes), the mass dependence of  $b_{sh}$  is very weak, at least at low masses. The same effect happens for luminosity dependence of galaxy clustering. For a fixed halo occupation, there is not a strong dependence of  $b_g$  on luminosity.

(v) The reconstructions of  $b_g(L)$  from  $b_{sh}(M)$  are better in highly occupied haloes than in haloes with no substructure. The problems of the reconstructions of  $b_g(L)$  come from the low mass objects, where the HOD assumptions does not work, since the clustering of galaxies does not show a clear dependence on halo or subhalo mass. At high masses, we find an agreement with the HOD assumptions.

(vi) The suppression of galaxies in the smallest haloes avoids the problems of the reconstructions of  $b_g(L)$ , but changes the shape of the luminosity dependence of  $b_g(L)$ , which makes it inconsistent with observations from SDSS DR7 (Zehavi et al. 2011). So, the HOD model seems to be

incompatible with the SAMs of the Millennium Simulation at low masses,  $M_h \lesssim 10^{11} M_\odot$ .

Although the limitations of the simulation do not allow us to analyse these reconstructions at large masses, the agreement between Tinker et al. (2010) and SMT (2001) models, together with the convergence of Figs. 14 and 16 at the largest masses studied, seem to indicate that the SAMs agree with the HOD model at large masses. However, there is no consistency between the HOD model and the SAMs on small masses. If these processes are reliable, then care must be taken when assuming the HOD model at masses below  $10^{11} M_\odot$ . Frequently, the HOD is assumed to relate galaxy properties and halo masses (Zehavi et al. 2011, Cooray et al. 2012). In the case of Zehavi et al. (2011), they measure the HOD parameters from the clustering of galaxies. If nature is in agreement with the SAMs, as the bright galaxies that reside in low mass haloes have a high clustering, then we would assume these haloes to be large, and we would be underestimating the number of small haloes with bright galaxies, and hence the HOD at these masses.

To show explicitly this problem, in Fig. 19 we compare different ways of measuring the reconstruction of  $b_g(L)$  from  $b_{mh}(M)$ . For the red dashed lines, the reconstructions are obtained from equation 4 but assuming the Tinker et al. (2010) model for the values of  $b_{mh}(M)$ , as in the blue dashed lines from Fig. 9. For the black dashed lines, we also assume Tinker et al. (2008) for the main halo mass function and Zehavi et al. (2011) for the HODs values. This is the reconstruction that is more related to the studies from observations, since we cannot observe the halo mass function and bias, and hence the HOD. In Fig. 19 we can see the differences obtained from the reconstructions depending on whether we assume or not the HOD. We can see that modelling  $b_{mh}(M)$  is not a problem (within 5% accuracy), but modelling the HOD produces important disagreements between the reconstructions and the real values of  $b_g(L)$ .

Recent studies (Tissera et al. 2010, Sawala et al. 2012) reflect the need to take into account baryonic effects on the dark matter haloes. The density profile of haloes change substantially when baryons are included, and this change can produce important effects on the galaxy formation models applied (Tissera et al. 2010). Sawala et al. (2012) also saw that baryonic physics reduces the mass and abundance of haloes below  $M_h < 10^{12}$ . Our study indicates that it would be premature to use the HOD interpretation for such halo masses to study these baryonic effects using the clustering of galaxies.

## ACKNOWLEDGEMENTS

We thank Marc Manera for interesting discussions and useful ideas. We also thank Carlton Baugh, Sergio Contreras, Qi Guo, Noelia Jiménez, Cedric Lacey and Ravi Sheth for their comments and discussions about this project. A.P. wants to thank also Albert Izzard for useful code support. The Millennium Simulation databases used in this paper and the web application providing online access to them were constructed as part of the activities of the German Astrophysical Virtual Observatory (GAVO). Funding for this

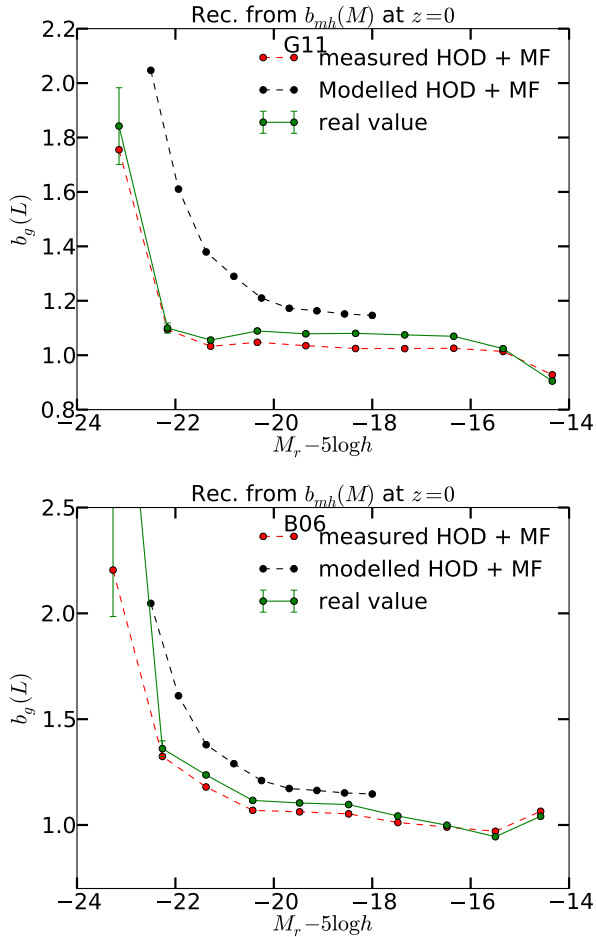


**Figure 19.** Reconstruction of  $b_g(L)$  from  $b_{mh}(M)$  for G11 (top) and B06 (bottom) models using all the galaxies in all the main halo masses. Solid green lines show the measured  $b_g(L)$  from the SAMs. Red dashed lines show the reconstructions assuming the Tinker et al. (2010) model for the values of  $b_{mh}(M)$ , as in the blue dashed lines from Fig. 9. Black dashed lines show the reconstructions obtained by assuming the Tinker et al. (2010) for the values of  $b_{mh}(M)$ , assuming the Tinker et al. (2008) model for the mass function of main haloes, and using the values of Zehavi et al. (2011) for the HODs.

project was partially provided by the Spanish Ministerio de Ciencia e Innovacion (MICINN), project AYA2009-13936, Consolider-Ingenio CSD2007- 00060, European Commission Marie Curie Initial Training Network CosmoComp (PITN-GA-2009-238356), research project 2009- SGR-1398 from Generalitat de Catalunya. A.P. was supported by beca FI from Generalitat de Catalunya.

## REFERENCES

Baugh C. M., 2006, Reports on Progress in Physics, 69, 3101  
 Baugh C. M., 2013, arXiv:1302.2768  
 Berlind A. A., & Weinberg D. H., 2002, ApJ, 575, 587

Bernardi M., Meert A., Sheth R. K., Vikram V., Huertas-Company M., Mei S., Shankar F., 2013, arXiv:1304.7778  
 Bertone S., De Lucia G., Thomas P. A., 2007, MNRAS, 379, 1143  
 Blanton M. R., Eisenstein D., Hogg D. W., Schlegel D. J., Brinkmann J., 2005, ApJ, 629, 143  
 Bower R. G., Benson A. J., Malbon R., Helly J. C., Frenk C. S., Baugh C. M., Cole S., Lacey C. G., 2006, MNRAS, 370, 645  
 Cole S., Lacey C. G., Baugh C. M., Frenk C. S., 2000, MNRAS, 319, 168  
 Cole S., et al., 2005, MNRAS, 362, 505-534  
 Conroy C., Wechsler R. H. & Kravtsov A. V., 2006, ApJ, 647, 201  
 Contreras S., Baugh C., Norberg P., Padilla N., 2013, arXiv:1301.3497  
 Cooray A., 2004, MNRAS, 348, 250  
 Cooray A., Gong Y., Smidt J., Santos M. G., 2012a, ApJ, 756, 92  
 Cooray A., Sheth R., 2002, PhysRep, 372, 1  
 Coupon J., Kilbinger M., McCracken H. J., Ilbert O., Arnouts S., Mellier T., Abbas U., de la Torre S., Goranova Y., Hudelot P., Kneib J.-P., Lefvre O., 2012, A & A, 542, A5  
 Croft R. A. C., Di Matteo T., Khandai N., Springel V., Jana A., Gardner J. P., 2012, MNRAS, 425, 2766  
 Croton D. J., Springel V., White S. D. M., De Lucia G., Frenk C. S., Gao L., Jenkins A., Kauffmann G., Navarro J. F., Yoshida N., 2006, MNRAS, 365, 11  
 De Lucia G., Blaizot J., 2007, MNRAS, 375, 2  
 Font A. S., Bower R. G., McCarthy I. G., Benson A. J., Frenk C. S., Helly J. C., Lacey C. G., Baugh C. M., Cole S., 2008, MNRAS, 389, 1619  
 Fry J. N., Gaztañaga E., 1993, ApJ, 413, 447  
 Fukugita M., Shimasaku K., Ichikawa T., 1995, PASP, 107, 945  
 Gao L., Springel V., White S. D. M., 2005, MNRAS, 363, L66  
 Geach J. E., Sobral D., Hickox R. C., Wake D. A., Smail I., Best P. N., Baugh C. M., Stott J. P., 2012, MNRAS, 426, 679  
 Governato, F., Babul, A., Quinn, T., Tozzi, P., Baugh, C. M., Katz, N., Lake, G., 1999, MNRAS, 307, 949  
 Gross M. A. K., Somerville R. S., Primack J. R., Holtzman J., Klypin A., 1998, MNRAS, 301, 81  
 Guo Q., White S., Boylan-Kolchin M., De Lucia G., Kauffmann G., Lemson G., Li C., Springel V., Weinmann S., 2011, MNRAS, 413, 101  
 Harker, G., Cole, S., Helly, J., Frenk, C. and Jenkins, A., 2006, MNRAS, 367, 1039  
 Hearin A. P., Zentner A. R., Berlind A. A., Newman J. A., 2012, arXiv:1210.4927  
 Helly J. C., Cole S., Frenk C. S., Baugh C. M., Benson A. J., Lacey C., 2003, MNRAS, 338, 903  
 Jenkins A., Frenk C. S., White S. D. M., Colberg J. M., Cole S., Evrard A. E., Couchman H. M. P., Yoshida N., 2001, MNRAS, 321, 372  
 Kauffmann G., Colberg J., Diaferio A., White S. D. M., 1999, MNRAS, 303, 188  
 Knebe A, Knollmann S. R., Muldrew S. I., et al. , 2011, MNRAS, 415, 2293  
 Kravtsov A. V., Berlind A. A., Wechsler R. H., Klypin A. A., Göttinger S., Allgood B., Primack J. R., 2004, ApJ, 609, 35  
 Lee J. & Shandarin S. F., 1999, ApJ, 517, L5  
 Merson A. I. et al., 2012, MNRAS, 342  
 Mo H. J., & White S. D. M., 1996, MNRAS, 282, 1096  
 Moster B. P., Somerville R. S., Maubetsch C., van den Bosch F. C., Macciò A. V., Naab T., Oser L., 2010, ApJ, 710, 903  
 Muldrew S. I., Pearce F. R., Power C., 2011, MNRAS, 410, 2617  
 Norberg P., Baugh C. M., Gaztanaga E., Croton D. J., 2009, MNRAS, 396, 19  
 Press W., Schechter P., 1974, ApJ, 304, 297

- Reddick R. M., Wechsler R. H., Tinker J. L., Behroozi P. S., 2012, arXiv:1207.2160
- Sawala T., Frenk C. S., Crain R. A., Jenkins A., Schaye J., Theuns T., Zavala J., 2012, arXiv:1206.6495
- Scoccimarro R., Sheth R. K., Hui L., Jain B., 2001, ApJ, 546, 20
- Seljak U. & Zaldarriaga M., 1996, ApJ, 469, 437
- Sheth R. K., Tormen G., 1999, MNRAS, 301, 119
- Sheth R. K., Diaferio A., Hui L., Scoccimarro R., 2001a, MNRAS, 326, 463
- Sheth R. K., Mo H. J., & Tormen G., 2001, MNRAS, 323, 1
- Simha V., Weinberg D., Dave R., Fardal M., Katz N., Oppenheimer B. D., 2010, arXiv:1011.4964
- Skibba R., Sheth R. K., Connolly A. J., Scranton R., 2006, MNRAS, 369, 68
- Smith R. E., Peacock J. A., Jenkins A., White S. D. M., Frenk C. S., Pearce F. R., Thomas P. A., Efstathiou G., Couchman H. M. P., 2003, MNRAS, 341, 1311
- Spergel D. N., Verde L., Peiris H. V., Komatsu E., et al. 2003, ApJS, 148, 175
- Springel V., White S. D. M., Tormen G., Kauffmann G., 2001, MNRAS, 328, 726
- Springel V., White S. D. M., Jenkins A., Frenk C. S., Yoshida N., Gao L., Navarro J., Thacker R., Croton D., Helly J., Peacock J. A., Cole S., Thomas P., Couchman H., Evrard A., Colberg J., Pearce F., 2005, Nature, 435, 629
- Tinker J., Kravtsov A. V., Klypin A., Abazajian K., Warren M., Yepes G., Gottlöber S., Holz D. E., 2008, ApJ, 688, 709
- Tinker J. L., Robertson B. E., Kravtsov A. V., Klypin A., Warren M. S., Yepes G., Gottlöber S., 2010, ApJ, 724, 878
- Tissera P. B., White S. D. M., Pedrosa S., Scannapieco C., 2010, MNRAS, 406, 922
- Trujillo-Gomez S., Klypin A., Primack J., Romanowsky A. J., 2011, ApJ, 742, 16
- Wake D. A., Franx M., van Dokkum P. G., 2012, arXiv:1201.1913
- Wechsler, R. H., Zentner, A. R., Bullock, J. S., Kravtsov, A. V. and Allgood, B., 2006, ApJ, 652, 71
- Xu A., 1995, ApJ, 98, 355
- Zehavi I., Zheng Z., Weinberg D. H., Frieman J. A., Berlind A. A. et al., 2005, ApJ, 630, 1
- Zehavi I., Zheng Z., Weinberg D. H., Blanton M. R., Bahcall N. A., Berlind A. A., Brinkmann J., Frieman J. A., Gunn J. E., Lupton R. H., Nichol R. C., Percival W. J., Schneider D. P., Skibba R. A., Strauss M. A., Tegmark M., York D. G., 2011, ApJ, 736, 59
- Zheng Z., Coil A. L. & Zehavi I., 2007, ApJ, 667, 760